Journal of Molecular Liquids

Experimental study of a hemispherical three-dimensional solar collector operating with silver-water nanofluid

--Manuscript Draft--

Manuscript Number:	MOLLIQ-D-20-00717
Article Type:	Full length article
Section/Category:	Colloidal solutions and nanoparticles
Keywords:	Solar collector; hemispherical collector; Ag-water nanofluid; efficiency
Corresponding Author:	Mohammad Hossein Doranehgard University of Alberta Edmonton, AB Canada
First Author:	Mojtaba Moravaj, PhD
Order of Authors:	Mojtaba Moravaj, PhD
	Mohammad Hossein Doranehgard
	Alireza Razeghizadeh
	Fatemeh Namdarnia
	Nader Karimi, PhD
	Larry K. B. Li, PhD
	Hamid Mozafari
Abstract:	In this experimental study, a fixed three-dimensional solar collector with a hemispherical geometry has been evaluated in accordance with ASHRAE standards. The solar collector features spiral tubes that transport fluid from the inlet to the outlet with no riser. Pure water and Ag-water nanofluid at different nanoparticle concentrations (0.1, 0.2 and 0 .3%) and different flow rates (0.1 to 0.6 GPM) were tested under different environmental conditions (temperature and radiation). The results show that the hemispherical solar collector, owing to its geometry and the specific arrangement of its pipes in relation to the overall surface area, exhibits promising thermal performance, making it a viable candidate for both domestic and industrial deployment. The average increase in efficiency when switching from water to Ag-water nanofluid was found to be around 11%, with the maximum efficiency (61.1%) attained at a nanoparticle concentration of 0.3% and a flow rate of 0.6 GPM.
Suggested Reviewers:	Rahmat Ellahi, PhD Professor, University of California Riverside rellahi@alumni.ucr.edu Prof. Ellahi is an expert in the field of renewable energy sources. He has many publications in this field
	Hafiz Ali, PhD Associate Professor, King Fahad University hafiz.ali@kfupm.edu.sa Dr. Ali is the Associate Editor of many ISI Journals and he is expert in the field of nanofluids.
	Saman Rashidi, PhD Associate Professor, Semnan University samanrashidi@semnan.ac.ir
	Mostafa Safdari Shadloo, PhD Associate Professor, INSA-Rouen: Institut National des Sciences Appliquees de Rouen msshadloo@coria.fr He has many publications in the field of application of nanofluids in the solar energy.
Opposed Reviewers:	

Mohammad Hossein Doranehgard
School of Petroleum and Mining Engineering
University of Alberta, T6G 2H5
Tel: +1 5149612550
doranehg@ualberta.ca

November 30, 2020

Dear Professor Vega

I am pleased to submit an original research article entitled "***Experimental study of a hemispherical three-dimensional solar collector operating with silver-water nanofluid***" for consideration in the Journal of Molecular Liquids.

This paper has not been published and is not under consideration for publication elsewhere. We have no conflicts of interest to disclose.

Thank you for your consideration.

Best regards,

Mohammad Hossein Doranehgard

Highlights

- A 3-D hemispherical solar collector was experimentally investigated
- Using Ag-water nanofluids, the performance of the collector was studied
- Effects of the flow conditions and ambient parameters evaluated on the efficiency

Experimental study of a hemispherical three-dimensional solar collector operating with silver-water nanofluid

Mojtaba Moravej [1], Mohammad Hossein Doranehgard [2*], Alireza Razeghizadeh [3], Fatemeh Namdarnia[1], Nader Karimi [4,5], Larry K. B. Li [6], Hamid Mozafari[1],

[1] Mechanical Engineering Department, Payame noor University, Iran.

[2] Department of Civil and Environmental Engineering, School of Mining and Petroleum Engineering, University of Alberta, Edmonton, Alberta T6G 1H9, Canada

[3] Science Department, Payame noor University, Iran.

[4] School of Engineering and Computer Science, Queen Mary University of London, Mile End, E1 4NS, UK

[5] James Watt School of Engineering, University of Glasgow, Glasgow, G12 8QQ, UK

[6] Department of Mechanical and Aerospace Engineering, Hong Kong University of Science and Technology, Clear Water Bay, Hong Kong

*Corresponding author (M. H. Doranehgard): doranehg@ualberta.ca

Abstract

In this experimental study, a fixed three-dimensional solar collector with a hemispherical geometry has been evaluated in accordance with ASHRAE standards. The solar collector features spiral tubes that transport fluid from the inlet to the outlet with no riser. Pure water and Ag-water nanofluid at different nanoparticle concentrations (0.1, 0.2 and 0.3%) and different flow rates (0.1 to 0.6 GPM) were tested under different environmental conditions (temperature and radiation). The results show that the hemispherical solar collector, owing to its geometry and the specific arrangement of its pipes in relation to the overall surface area, exhibits promising thermal performance, making it a viable candidate for both domestic and industrial deployment. The average increase in efficiency when switching from water to Ag-water nanofluid was found to be around 11%, with the maximum efficiency (61.1%) attained at a nanoparticle concentration of 0.3% and a flow rate of 0.6 GPM.

Keywords: Solar collector, hemispherical collector, Ag- water nanofluid, efficiency

1. Introduction

Easy and cheap access to solar energy has made it one of the most promising sources of renewable energy. Solar energy can be divided into three main types based on their application: light, electric and thermal. In solar thermal energy, the sun's radiant energy is transferred to an intermediate fluid such as water or air in a device called a solar collector, and then this thermal energy is transferred to the desired location or material. Solar collectors come in various forms, the simplest of which is the flat plate collector, which can feature different designs and geometries [1-3]. If more heat could be transferred from the solar radiation reaching the collector to the operating fluid, the efficiency and performance of the collector would increase. Various factors can influence this, including the absorber geometry and materials, the characteristics of the tubes transporting the operating fluid, the fluid type, coatings and various other factors. Increasing the efficiency of flat plate collectors has been the subject of considerable research [4-6]. Saffarian *et al*. [7] theoretically evaluated a flat plate collector in terms of its pipe arrangement and factors such as the pressure drop, heat transfer coefficient and efficiency. These researchers showed that the use of a U-shaped pipe arrangement can lead to better performance than other geometries [7].

Noghreabadi *et al*. [8] experimentally examined a three-dimensional solar collector with conical geometry. The collector adsorbent was a conical shell in which the operating fluid pipes were connected to the adsorbent in a spiral from the bottom to top. The results of this study showed promising thermal performance and a maximum efficiency of 65% [8]. Moravej *et al*. [9] experimentally tested a circular flat plate collector under the ASHRAE standard. In this collector, the pipes were woven in a spiral in the absorber circle from the margin to the center of the circle, and after this path, the fluid exited in the center, under the collector. The results of this study revealed a significant increase in efficiency, especially at high fluid velocities.

Another effective way of increasing the efficiency of flat plate collectors, which has been widely studied by researchers in recent years, is to use nanofluids instead of ordinary water as the operating fluid. Zayed *et al*. [10] examined solar flat panel collectors operating with nanofluids for improved efficiency, and found that the best nanofluid was copper oxide. In most studies, this nanofluid was used in the concentration range of 0.25 to 2% and flow rates of 8.8 to 1 GPM, and the observed increase in efficiency was around 3.37 to 3.6%.

Sharafuddin [11] conducted an experimental study of solar collectors using water in three different concentrations, with a nanoparticle size of about 40 nm, and showed that the efficiency can increase to 10.74%. Lee et al. [12] investigated the effect of the specific heat and photothermal conversions on solar collector performance using modified carbon nanotubes (CD-CNTs) of β-cyclodextrin. Different concentrations were used in different conditions, and the conclusion was that the specific heat capacity increases by more than 9% for each 0.1% increment in concentration.

Sundar et al. [13] carried out an analysis of a flat plate solar collector with the use of nanofluids as the operating fluid. Issues such as economic value due to dimensional reduction, heat transfer measurement and collector efficiency were investigated in different wire winding models. The results showed that using this model of coil wire reduces the dimensions of the solar collector by about 27.66% for water as the working fluid, and by about 39.33% for water-alumina nanofluid at a concentration of 0.3%.

In another study, Moravej *et al.* [14] experimentally investigated the increase in efficiency of a square flat plate solar collector using water, nanoparticles and titanium dioxide of the rutile type. The maximum efficiency reported was around 78%. Sakhaei and Valipour [15] conducted an experimental study on the thermal performance and heat transfer parameters of a flat plate solar collector featuring helical risers. Mirzaei [16] experimentally examined the effect of nanofluid addition on the thermal performance of a flat plate collector at different flow rates; a quadratic function was used to estimate the coefficient of performance and loss coefficient. An efficiency increase of up to 80% was found at a flow rate of 4 LPM.

In the present research, we experimentally examine a flat plate solar collector with hemispherical geometry and no riser. We designed and built this configuration, which features a zig-zag tube arrangement, specifically for use in various conditions, including different temperatures and operating fluids such as ordinary water and silver-water nanofluid. We focus on testing three different nanoparticle concentrations based on the ASHRAE standard.

2- Materials and methods

2-1-Collector configuration

The collector used in this research is a fixed three-dimensional solar collector, which has a protruding hemispherical absorber to which the tubes containing the working fluid are connected. The fluid inlet is from the side and exits the collector after a spiral path. The glass cover of this collector is dome-shaped, below which is an insulation plate. The technical specifications and features of the hemispherical collector, including its dimensions and materials, are listed in Table 1. The ASHRAE standard was used to perform the tests, and the laboratory layout and location of the equipment are shown in Figure 1.

Table 1 Specifications of the hemispherical solar collector

Parts	Properties	Values	Units
Glass cover	Thickness	6	mm
	Conduction coefficient	12.1	w/m.°c
	Density	2200	g/cm^3
	Specific heat	670	J/kg.°c
	Reflection coefficient	0.0794	-
	Absorption coefficient	0386.0	-
	Diffusion coefficient	526.1	-
Absorber	Area	1	m^2
	Conduction coefficient	4.80	w/m.°c
	Specific heat	10.25	J/kg.°c
	Density	87.37	g/cm^3
	Absorption coefficient	9.0	
Piping	Copper pipe	9.6	mm
Insulation	Polyester wall insulation	20	mm
	Insulation of the bottom plastofoam	20	mm

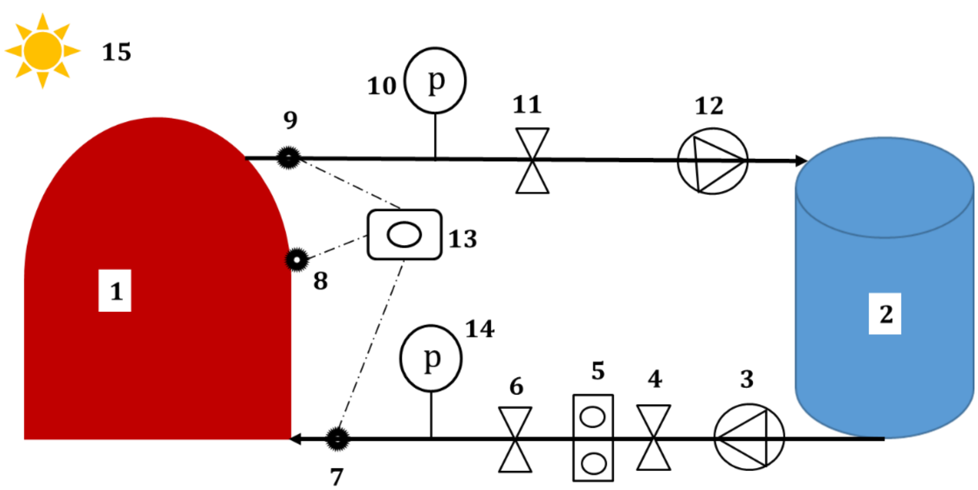

1	Hemispherical collector	5	Rota meter
2	Tank	6	Control valve
3,12	Water pump	7,8,9	Thermocouples
4,11	Flow valves	10,14	Pressure gauge
15	Sun	13	Data logger

Figure 1 Experimental configuration

Figure 2 is a photograph of the experimental setup, which includes a hemisphere solar collector at the test site in Payame Noor Aghajari University. Experiments were performed in different conditions and on different days, and the results were analyzed. Table 2 also represents the uncertainty for different parameter.

Figure 2 Photo of the hemispherical solar collector during an experimental run.

Table 2 Measuring devices and instruments

Parameter	**Model**	**Uncertainty**	**Units**
Temperature	Lutron	0.1	^{0} C
Flow rate	Km450	0.1	gpm
Wind speed	Lutron	0.1	m/s
Radiation	Tes-132	1	W/m^2
Humidity	Htc-110	1	%

Table 3 lists the ASHRAE standards for testing solar collectors. The fluid flow rate, inlet temperature and pressure are recorded at the inlet. After the operating fluid enters the collector and travels through a spiral path in the hemispherical collector, it exits from the top and at the outlet, where the temperature and pressure are measured, and then the fluid returns to the storage tank. This cycle repeats itself. The temperature, humidity and wind speed are also measured separately. To accurately collect data in accordance with the ASHRAE standard, one should determine the solar collector performance in stable or quasi-stable conditions. In other words, the actual efficiency of the collector should be measured only when it is relatively stable in terms of thermal equilibrium and saturation. The amount of time required to reach this state is based on a fixed time criterion according to Equation (1).

Table 3 ASHRAE standards.

Variable	**Absolute limits**
Total solar irradiance normal to sun(W/m^2)	790 (minimum)
Diffuse fraction (%)	20
Wind speed	2.3 < U < 4.8
Incidence angle modifier	98%<normal incidence, value<102%

2-3-Nanofluid preparation

Nanofluids can be prepared from nanoparticles in two different methods: single-stage and two-stage. Nowadays, the latter method is more common. In addition to determining the preparation method, the degree of stability and proper dispersion of nanoparticles in the nanofluid are two key considerations. In the present study, silver nanoparticles with a purity of 99.99% and a size between 5 to 8 nm were used to prepare silver-water nanofluids at three different concentrations: 0.1, 0.2 and 0.3%. These nanoparticles are Model Number US7150 and are mixed with deionized water. The distribution is prepared by ultrasonic device (Nano Sadra Company). Figure 3 shows photographs of the nanofluids, and Figure 4 shows a TEM image. Before an experiment, measurements of clustering and visual stability were performed. The physical characteristics of the nanoparticles and base liquid are listed in Table 4.

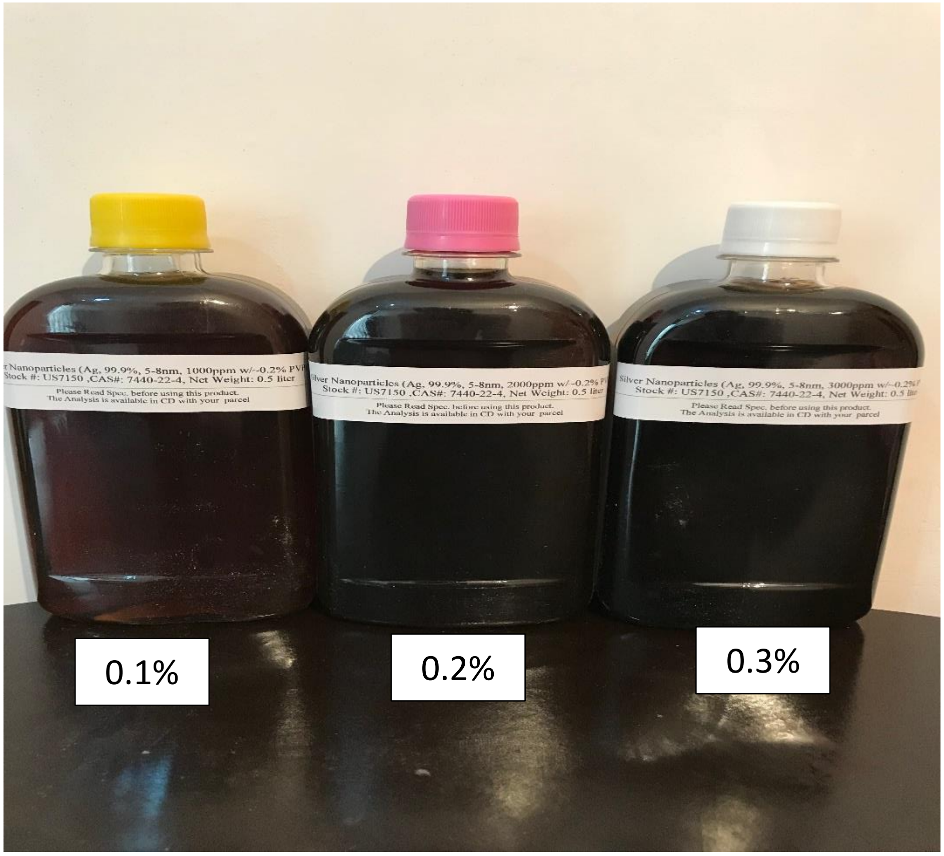

Figure 3 Silver-water nanofluid with different concentrations

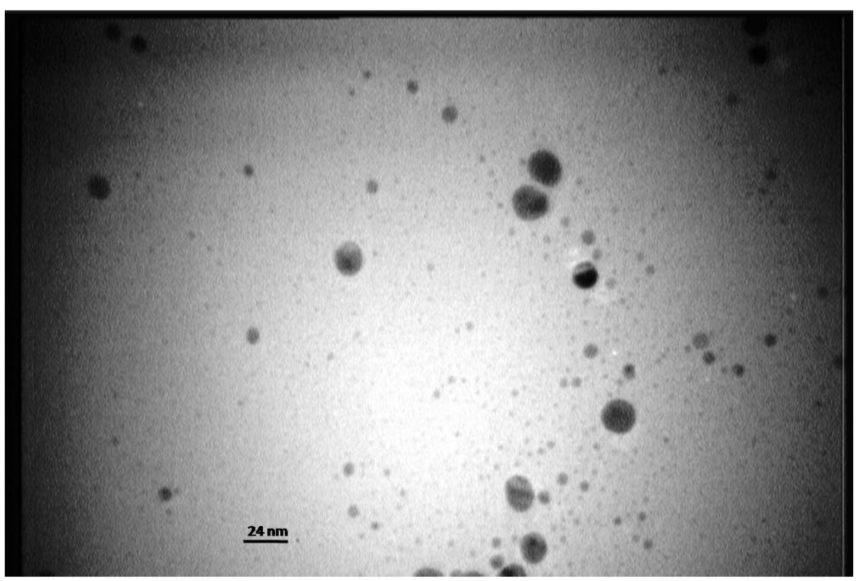

Figure 4 TEM image of 0.3wt% Ag-water nanofluid

Table 4 Physical characteristics of the base fluid and nanoparticles

Materials	C_P(J/kg K)	K (W/m K)	ρ (W/m^3)
Water	4180	0.613	998
Nanoparticle	880	35	3890

2-4-Governing parameters

One of the evaluation criteria of solar collectors is their efficiency, which is calculated as the ratio between the useful thermal energy extracted and the amount of solar radiation received. According to the ASHRAE standard used in this study, the thermal performance of the collector at different fluid inlet temperatures should be investigated. Equation (1) can be used to calculate the useful energy obtained from the collector:

$$\mathrm{Q_u} = E_{out} - E_{in} \tag{1}$$

$$\mathrm{Q_u} = \dot{\mathrm{m}}\mathrm{C_p}(\mathrm{T_o} - \mathrm{T_i}) \tag{2}$$

$$\mathrm{F_R} = \frac{\dot{\mathrm{m}}\mathrm{C_p}(\mathrm{T_o} - \mathrm{T_i})}{\mathrm{A_c}[\mathrm{G_T}(\tau\alpha) - \mathrm{U_L}(\mathrm{T_i} - \mathrm{T_a})]} \tag{3}$$

Therefore, the amount of useful energy extracted from the collector can be found as follows [8, 19]:

$$\mathrm{Q_u} = \mathrm{A_p}\mathrm{F_R}[\mathrm{Rad} - \mathrm{U_l}(\mathrm{T_{in}} - \mathrm{T_a})] \tag{4}$$

The useful energy extracted from the collector is equal to the amount of heat transferred to the working fluid, which can be calculated from the specific heat value of the liquid at its pre-boiling temperature. The specific heat of the nanofluid can be calculated from Equation (5) [14,15,17]:

$$\mathrm{C_{p,nf}} = \mathrm{C_{p,np}}(\varphi) + \mathrm{C_{p,bf}}\,(1 - \varphi) \tag{5}$$

where $C_{p,nf}$ is the heat capacity of the nanofluid, $C_{p,np}$ is the heat capacity of the nanoparticles, φ is the volume fraction of the nanoparticles, and $C_{p,bf}$ is the heat capacity of water as the base liquid. Because the energy reaching the collector is the same as the solar energy, the collector efficiency can be found via Equation (6) [19]:

$$\eta_{\mathrm{i}} = \frac{Q_u}{\mathrm{A_c}Rad} = \frac{\dot{m}C_p(T_o - T_i)}{\mathrm{A_c}Rad} \tag{6}$$

According to Equations (3) and (6), the collector efficiency can be written as Equation (7) [19]:

$$\eta_{\mathrm{i}} = \mathrm{F_R}(\tau\alpha) - \mathrm{F_R}\mathrm{U_L}\left(\frac{\mathrm{T_i} - \mathrm{T_a}}{Rad}\right) \tag{7}$$

According to Equation (7), if the return values are plotted as a function of the variable $\frac{T_i - T_a}{Rad}$, the resulting curve forms a line whose intersection with the vertical axis is $\mathrm{F_R}$ (τα). This value indicates the maximum collector efficiency and occurs when the temperature of the fluid entering the collector is equal to the ambient temperature. The intersection of this line with the horizontal axis is called the collector static point, where the cumulative efficiency reaches zero and occurs when the flow velocity in the flow stream becomes zero. The slope of the line is $F_R U_L$, which represents the amount of energy lost [19].

2-5-Uncertainty analysis

The error sources in the present study include device calibration error, visual reading of figures as well as the type of devices used. Data errors include temperature, solar radiation, surface area, and flow rate. To calculate the uncertainty of the experiments, the square root (RSSM) method is used, which is presented in Equation (8) [6-9].

$$\mathrm{S} = \sqrt[2]{(\frac{\Delta \mathrm{u_1}}{\mathrm{u_1}})^2 + (\frac{\Delta \mathrm{u_2}}{\mathrm{u_2}})^2 + (\frac{\Delta \mathrm{u_3}}{\mathrm{u}})^2 + \cdots} \tag{8}$$

Therefore, to calculate the uncertainty of these measurements, the following equation can be written:

$$\mathrm{S_\eta} = \sqrt[2]{(\frac{\Delta \dot{\mathrm{m}}}{\dot{\mathrm{m}}})^2 + (\frac{\Delta \mathrm{DA}}{\mathrm{DA}})^2 + (\frac{\Delta \mathrm{DT}}{\mathrm{DT}})^2 + (\frac{\Delta \mathrm{G_T}}{\mathrm{G_T}})^2} \tag{9}$$

The uncertainty for the above values of current, area, temperature and solar radiation are 5.5, 0.01, 0.2 and 1.3 percent, respectively. From Equation (9), this implies an uncertainty in the efficiency of about 6.3%.

3. Results and discussion

In accordance with the ASHRAE standard, tests were performed on different days and under different conditions. To achieve stable conditions of the collector and to perform the test with water and nanofluid in different concentrations, we start the test before noon and end it after three hours. Data collection is done every 20 minutes, which is a suitable time period both in terms of achieving the necessary time constant and quasi-stability of the collector and considering that some data such as the wind speed, temperature and humidity had to be read manually.

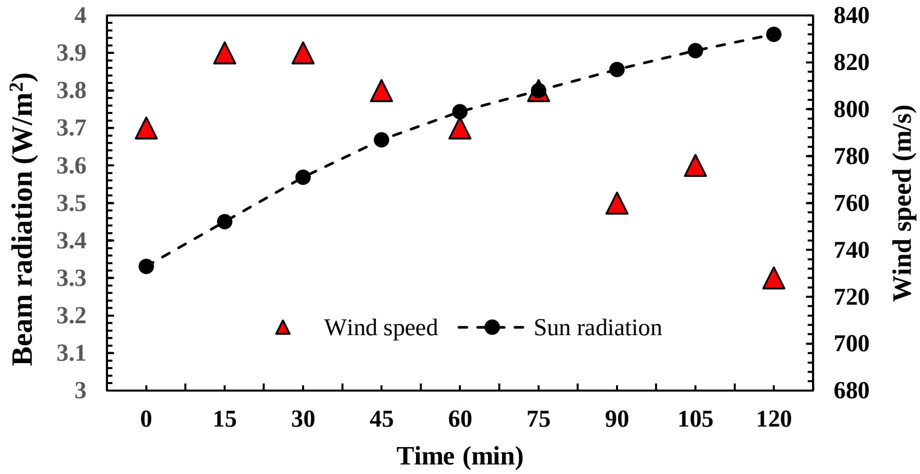

Figure 5 Solar radiation and wind speed during the experiment.

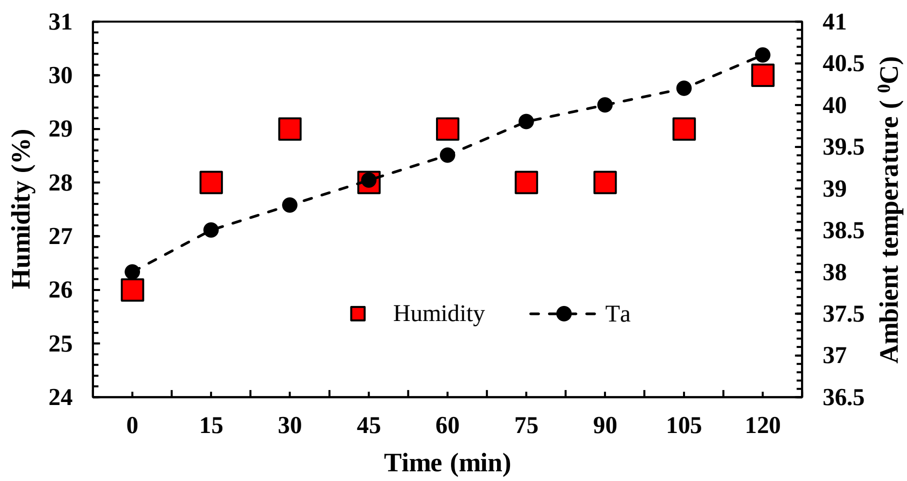

Figure 6 Ambient temperature and humidity during an experiment.

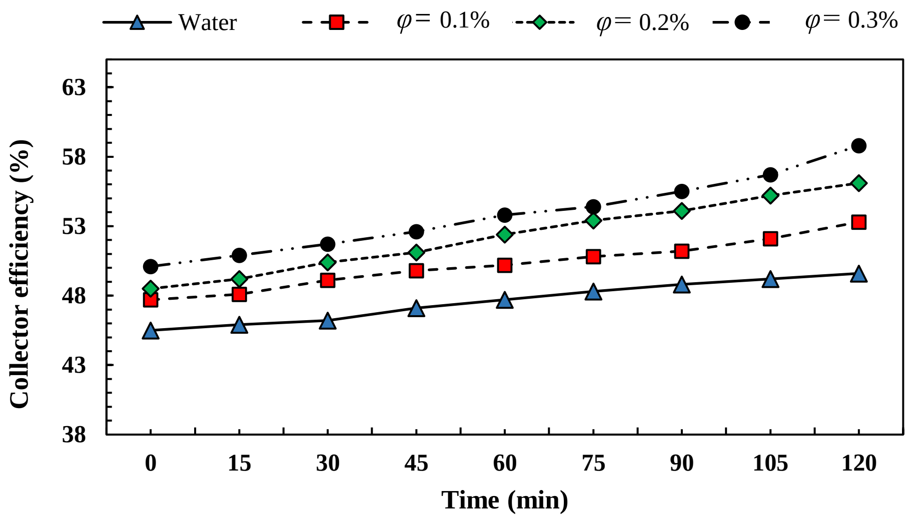

Figure 7 Collector efficiency for different working fluids during an experiment.

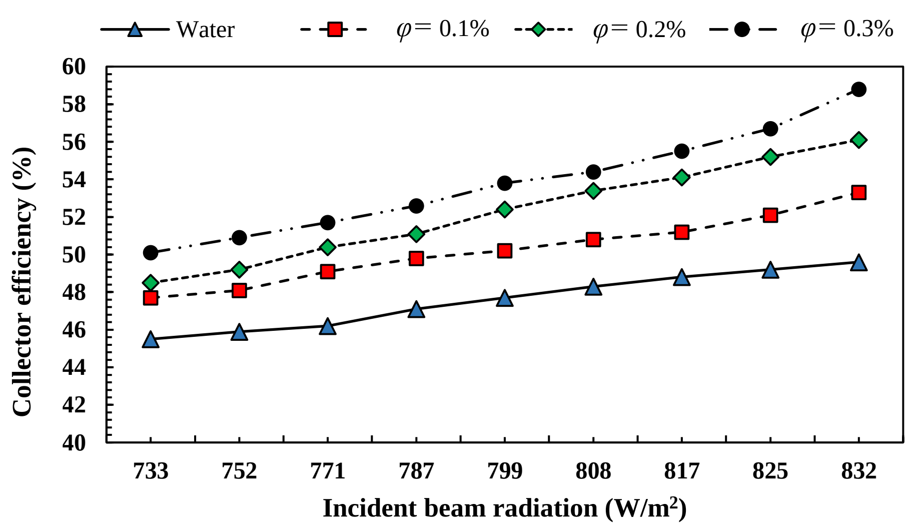

Figure 8 Collector efficiency for different working fluids as a function of solar radiation.

Figure 5 shows the solar radiation and wind speed around the collector during a test. It is apparent that the amount of solar radiation increases throughout the experiment, which is consistent with the fact that the experiments began before noon. The maximum solar radiation recorded at the test site was 902 W/m^2. Shown on the left axis of Figure 5 is the wind speed. A unique feature of this collector is its physical stability against wind as compared with rectangular collectors.

Figure 6 shows the ambient temperature and relative humidity at the test site, which was sunny and cloudless. The humidity remained relatively constant during the test, averaging at around 28%. The ambient air temperature rose during the test owing to the strong radiation and summer season. Figure 7 shows the efficiency of the collector during the test. Using nanofluids instead of water led to improvements in efficiency, with the efficiency increasing as the nanoparticle concentration increases.

Figure 8 shows the efficiency of the collector as a function of solar radiation. As the radiation increases, so does the efficiency, for both water and nanofluid as the working fluid. This increase in efficiency becomes larger with increasing nanoparticle concentration. This is due to the temperature-induced movements in nanoparticles, which increase with increasing radiation and consequently the temperature of the pipe wall, and thus the efficiency also increases.

Figure 9 shows the temperature difference between the output-input of the collector for water-working fluid and silver-water nanofluid at all three concentrations. With increasing time and radiation, and as a result of the inlet temperature and the temperature of the adsorbent and pipes, the rate of heat transfer increases for all cases.

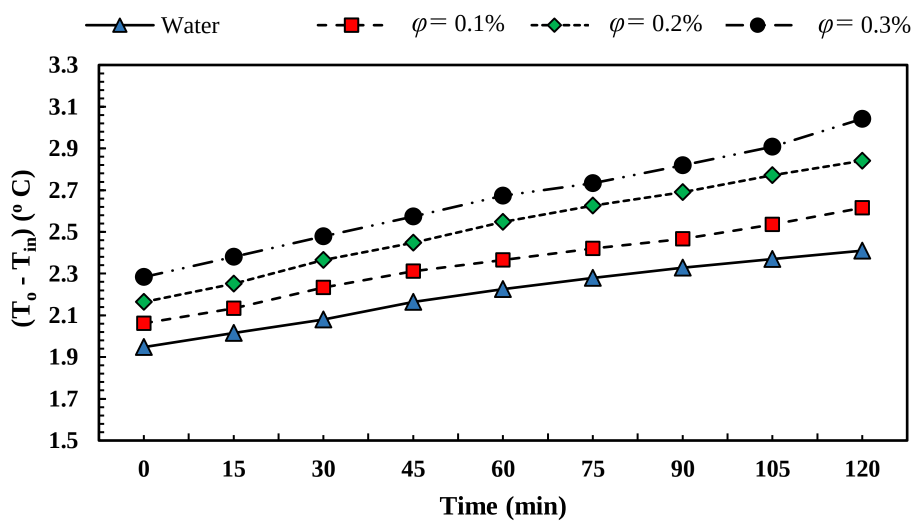

Figure 9: Output-inlet temperature in a hemispherical collector using water fluid and nanofluid at different concentrations.

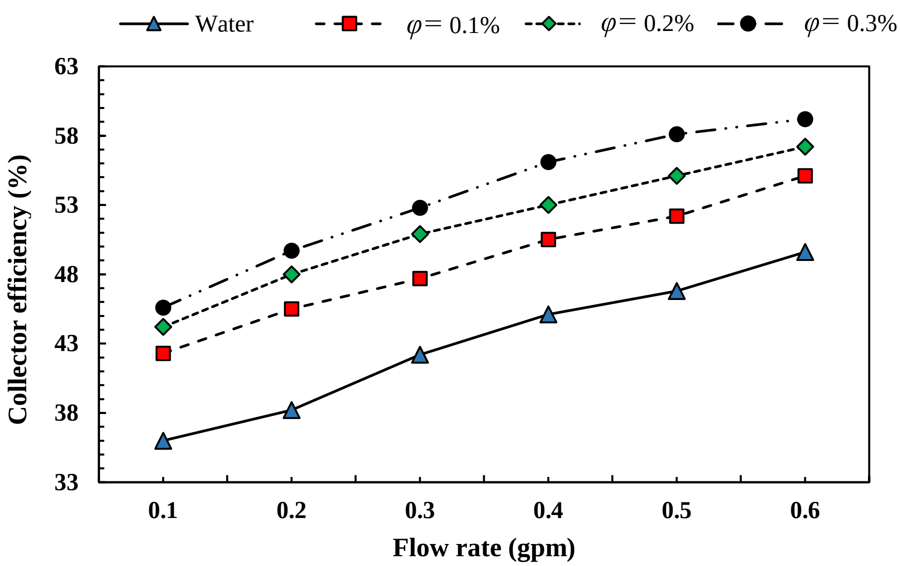

Figure 10 Collector efficiency as a function of flow rate for different working fluids.

Figure 10 shows the effect of flow rate on the efficiency of the collector. As the flow rate increases, for both water and nanofluid, the collector efficiency increases. Moreover, the efficiency also increases when switching from water to nanofluid, and with increasing nanoparticle concentration. This occurs because increasing the flow rate increases the Reynolds number, thus increasing the heat transfer to the fluid, resulting in an increase in efficiency. However, when using nanofluids, in addition to the direct effect of the Reynolds number, the movements of suspended nanoparticles such as Brownian motion have a direct effect on the heat transfer to the operating fluid.

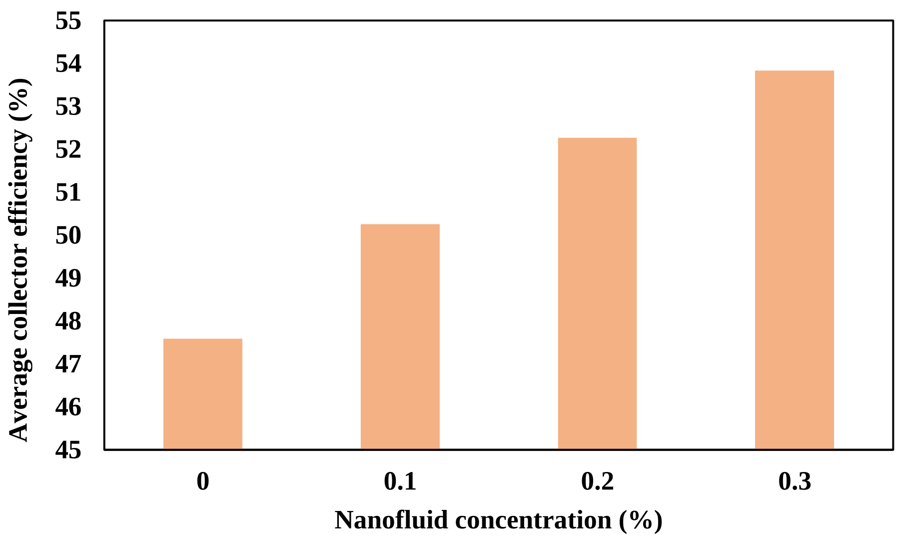

Figure 11 Collector efficiency as a function of nanoparticle concentration.

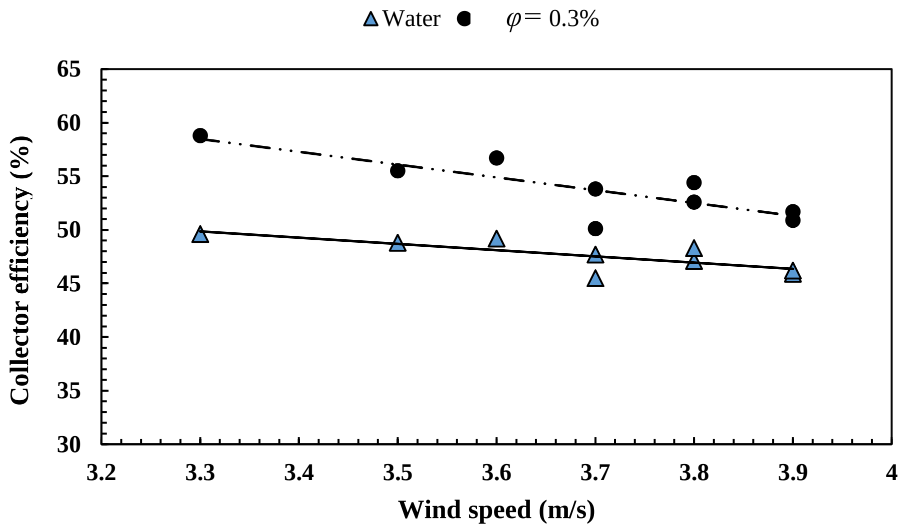

Figure 12 Collector efficiency as a function of wind speed for water and 0.3% of nanofluid.

Figure 11 shows the average collector efficiency as a function of the nanoparticle concentration. A significant efficiency increase arises from the use of nanofluids, as compared to the use of ordinary water, as the operating fluid. There is an efficiency increase of more than 11% in water. Figure 12 examines the effect of wind speed on collector efficiency. It is found that, as the wind speed increases, the collector efficiency decreases for both water and nanofluid, which can be attributed to the increase in heat loss around the collector.

4-Conclusions

In this experimental study, a hemispherical solar collector without a riser has been studied in accordance with ASHRAE standards. Experiments were performed using water and nanofluid as the operating fluids, at nanoparticle concentrations of 0.1, 0.2 and 0.3% for different flow rates and different environmental conditions. The results of this study can be summarized as follows:

- The hemispherical collector has the same behavior as conventional water heaters in terms of the parameters affecting the collector efficiency.
- The use of nanofluid increases the collector efficiency, with higher nanoparticle concentrations (from 0.1 to 0.3%) leading to higher efficiencies.

- With water and nanofluids as the operating fluid, the collector efficiency increases with increasing radiation, but its growth is higher for nanofluids because of the nanoparticles' effects at high temperatures.
- As the flow rate increases, so does the Reynolds number, causing the collector efficiency to increase as well, but when using nanofluids, especially higher nanoparticle concentrations, a significant increase in efficiency occurs owing to the increase in unpredictable movements of nanoparticles, including Brownian motion.
- The maximum collector efficiency recorded for the collector was 61.1%, and the average efficiency difference between the use of water or nanofluid was more than 11%.

Nomenclature

Parameter	Specification	Unit
A_p	Absorber area	(m^2)
C_p	Specific heat for fluid	(J/Kg k)
$C_{p,nf}$	Specific heat for nsnofluid	(J/Kg k)
$C_{p,np}$	Specific heat for nanoparticles	(J/Kg k)
$C_{p,bf}$	Specific heat for basefluid	(J/Kg k)
DT	Difference between inlet-outlet temperaure	$(^0 C)$
F_R	Coefficient of energy in collector	-
F'	Collector coefficient	-
Rad	Incident sun radiation	(W/m^2)
$\dot{m}$	Mass flow rate	(Kg/s)
Q_u	Useful energy gained from collector	(W)
S_η	Uncertainty	%
T_a	Ambient temperature	$(^0 C)$
T_{in}	Inlet temperature to the collector	$(^0 C)$
T_{out}	outlet temperature of the collector	$(^0 C)$
T_P	Absorber temperature	$(^0 C)$
U_L	Total loss energy coefficient	$(W/m^2 K)$
$T\alpha$	Absorption-transmittance product	-
μ	Nanofluid concentration	%
η_i	Instantaneous collector efficiency	%

References

[1] Rezvanpour, M., Borooghani, D., Torabi, F., & Pazoki, M. Using CaCl2· 6H2O as a phase change material for thermo-regulation and enhancing photovoltaic panels' conversion efficiency:

Experimental study and TRNSYS validation. *Renewable Energy,* Vol. *146,* (2020), 1907-1921. https://doi.org/10.1016/j.renene.2019.07.075

[2] Noghrehabadi, A., Hajidavalloo, E., & Moravej, M. Experimental investigation of efficiency of square flat-plate solar collector using SiO2/water nanofluid. *Case Studies in Thermal Engineering*, Vol. *8*, (2016), 378-386. https://doi.org/10.1016/j.csite.2016.08.006

[3] Elsheikh, A. H., Sharshir, S. W., Mostafa, M. E., Essa, F. A., & Ali, M. K. A. Applications of nanofluids in solar energy: a review of recent advances. *Renewable and Sustainable Energy Reviews*, Vol. *82*, (2018), 3483-3502. https://doi.org/10.1016/j.rser.2017.10.108

[4] Ahmed, O. K. A numerical and experimental investigation for a triangular storage collector. *Solar Energy*, Vol. *171*, (2018), 884-892. https://doi.org/10.1016/j.solener.2018.06.097

[5] Sint, N. K. C., Choudhury, I. A., Masjuki, H. H., & Aoyama, H. Theoretical analysis to determine the efficiency of a CuO-water nanofluid based-flat plate solar collector for domestic solar water heating system in Myanmar. *Solar Energy*, Vol. *155*, (2017), 608-619.https://doi.org/10.1016/j.solener.2017.06.055

[6] Noghrehabadi, A. R., Hajidavalloo, E., & Moravej, M. An experimental investigation on the performance of a symmetric conical solar collector using SiO2/water nanofluid. *Transp Phenom Nano Micro Scales*, Vol. *5, No. 1*, (2016), 23-29. DOI: 10.7508/tpnms.2017.01.003

[7] Saffarian, M. R., Moravej, M., & Doranehgard, M. H. Heat transfer enhancement in a flat plate solar collector with different flow path shapes using nanofluid. *Renewable Energy*, Vol. *146*, (2020), 2316-2329. https://doi.org/10.1016/j.renene.2019.08.081

[8] Noghrehabadi, A., Hajidavalloo, E., & Moravej, M. An experimental investigation of performance of a 3-D solar conical collector at different flow rates. *Journal of Heat and Mass Transfer Research*, Vol. *3*, No. 1, (2016), 57-66. DOI: 10.22075/JHMTR.2016.477

[9] Moravej, M., Saffarian, M. R., Li, L. K., Doranehgard, M. H., & Xiong, Q. Experimental investigation of circular flat-panel collector performance with spiral pipes. *Journal of Thermal Analysis and Calorimetry*, (2019), 1-8. https://doi.org/10.1007/s10973-019-08879-1

[10] Zayed, M. E., Zhao, J., Du, Y., Kabeel, A. E., & Shalaby, S. M. Factors affecting the thermal performance of the flat plate solar collector using nanofluids: a review. *Solar Energy*, Vol. *182*, (2019), 382-396. https://doi.org/10.1016/j.solener.2019.02.054

[11] Sharafeldin, M. A., & Gróf, G. Experimental investigation of flat plate solar collector using CeO2-water nanofluid. *Energy conversion and management*, Vol. *155*, (2018) 32-41. https://doi.org/10.1016/j.enconman.2017.10.070

[12] Li, X., Chen, W., & Zou, C. An experimental study on β-cyclodextrin modified carbon nanotubes nanofluids for the direct absorption solar collector (DASC): Specific heat capacity and photo-thermal conversion performance. *Solar Energy Materials and Solar Cells*, *204*, (2020) 110240. https://doi.org/10.1016/j.solmat.2019.110240

[13] Sundar, L. S., Sintie, Y. T., Said, Z., Singh, M. K., Punnaiah, V., & Sousa, A. C. (2020). Energy, efficiency, economic impact, and heat transfer aspects of solar flat plate collector with Al2O3 nanofluids and wire coil with core rod inserts. *Sustainable Energy Technologies and Assessments*, *40*, 100772. https://doi.org/10.1016/j.seta.2020.100772

[14] Moravej, M., Bozorg, M. V., Guan, Y., Li, L. K., Doranehgard, M. H., Hong, K., & Xiong, Q. (2020). Enhancing the efficiency of a symmetric flat-plate solar collector via the use of rutile TiO2-water nanofluids. Sustainable Energy Technologies and Assessments, Vol. 40, (2020), 100783. https://doi.org/10.1016/j.seta.2020.100783

[15] Sakhaei, S. A., & Valipour, M. S. Thermal performance analysis of a flat plate solar collector by utilizing helically corrugated risers: An experimental study. *Solar Energy*, Vol. *207*, (2020), 235-246. https://doi.org/10.1016/j.solener.2020.06.023

[16] Mirzaei, M. Experimental investigation of CuO nanofluid in the thermal characteristics of a flat plate solar collector. *Environmental Progress & Sustainable Energy*, Vol. *38, No. 1*, (2019), 260-267. https://doi.org/10.1002/ep.12902

[18] ASHRAE, Standard 93-2010– Methods of Testing to Determine the Thermal Performance of Solar Collectors (ANSI Approved), ANSI/ASHRAE Standard 93-2010 (R2014). ASHRAE Inc., Atlanta, USA. www.ASHRAE.org.

[19] Duffie, J. A., Beckman, W. A., & Blair, N.*Solar engineering of thermal processes, photovoltaics and wind*. John Wiley & Sons, (2020).

[20]Yousefi, T., Veysi, F., Shojaeizadeh, E., & Zinadini, S. An experimental investigation on the effect of Al2O3–H2O nanofluid on the efficiency of flat-plate solar collectors. *Renewable Energy*, Vol. *39, No. 1,* (2012), 293-298. https://doi.org/10.1016/j.renene.2011.08.056

[21]Gupta, H. K., Agrawal, G. D., & Mathur, J. Investigations for effect of Al2O3–H2O nanofluid flow rate on the efficiency of direct absorption solar collector. *Case Studies in Thermal Engineering*, Vol. *5*, (2015), 70-78. https://doi.org/10.1016/j.csite.2015.01.002

[22] Farajzadeh, E., Movahed, S., & Hosseini, R. Experimental and numerical investigations on the effect of Al2O3/TiO2H2O nanofluids on thermal efficiency of the flat plate solar collector. *Renewable Energy*, Vol. *118*, (2018), 122-130. https://doi.org/10.1016/j.renene.2017.10.102

[24] Rajput, N. S., Shukla, D. D., Rajput, D., & Sharm, S. K. Performance analysis of flat plate solar collector using Al2O3/distilled water nanofluid: an experimental investigation. *Materials Today: Proceedings*, Vol. *10*, (2019), 52-59. https://doi.org/10.1016/j.matpr.2019.02.188

[24] Hawwash, A. A., Rahman, A. K. A., Nada, S. A., & Ookawara, S. Numerical investigation and experimental verification of performance enhancement of flat plate solar collector using nanofluids. *Applied Thermal Engineering*, Vol. *130*, (2018), 363-374. https://doi.org/10.1016/j.applthermaleng.2017.11.027

[25] Hajabdollahi, F., & Premnath, K. Numerical study of the effect of nanoparticles on thermoeconomic improvement of a solar flat plate collector. *Applied Thermal Engineering*, Vol. *127*, (2017), 390-401. https://doi.org/10.1016/j.applthermaleng.2017.08.058

[26] Colangelo, G., Favale, E., De Risi, A., & Laforgia, D. A new solution for reduced sedimentation flat panel solar thermal collector using nanofluids. *Applied Energy*, Vol. *111*, (2013), 80-93. https://doi.org/10.1016/j.apenergy.2013.04.069

[27] Sundar, L. S., Singh, M. K., Punnaiah, V., & Sousa, A. C. Experimental investigation of Al2O3/water nanofluids on the effectiveness of solar flat-plate collectors with and without twisted tape inserts. *Renewable energy*, Vol. *119*, (2018), 820-833. https://doi.org/10.1016/j.renene.2017.10.056

Declaration of interests

☒ The authors declare that they have no known competing financial interests or personal relationships that could have appeared to influence the work reported in this paper.

☐The authors declare the following financial interests/personal relationships which may be considered as potential competing interests: